Exploration Geophysics (2006) ***37****, 44-49*
Butsuri-Tansa (Vol. 59, No. 1)
Mulli-Tamsa (Vol. 9, No. 1)

Monitoring CO_2 injection with cross-hole electrical resistivity tomography

N.B. Christensen D. Sherlock K. Dodds

Key Words: CO_2 sequestration, electrical resistivity tomography, monitoring, model study

ABSTRACT

In this study, the resolution capabilities of electrical resistivity tomography (ERT) in the monitoring of CO_2 injection are investigated. The pole-pole and bipole-bipole electrode configuration types are used between two uncased boreholes straddling the CO_2 plume. Forward responses for an initial pre-injection model and three models for subsequent stages of CO_2 injection are calculated for the two different electrode configuration types, noise is added and the theoretical data are inverted with both L1- and L2-norm optimisation.

The results show that CO_2 volumes over a certain threshold can be detected with confidence. The L1-norm proved superior to the L2-norm in most instances. Normalisation of the inverted models with the pre-injection inverse model gives good images of the regions of changing resistivity, and an integrated measure of the total change in resistivity proves to be a valid measure of the total injected volume.

INTRODUCTION

It is evident that injection of CO_2 cannot be monitored with surface electrical or electromagnetic measurements, as the spatial extent and the contrast in resistivity of the injected CO_2 would be much too small. However, better resolution can be obtained with electrical resistivity tomography (ERT), which is a technique for imaging the subsurface electrical structure using galvanic electrical measurements between electrodes in two boreholes. ERT has been used for many different purposes and it is a well studied and published subject in geophysics (e.g., Daily and Ramirez, 2000). Within the last 20 years, data acquisition hardware and inversion algorithms have improved rapidly to handle new challenges. In the following preliminary study, the application of ERT to the Otway Basin Pilot Program (OBPP) is considered with regard to electrode arrays, specific configurations, and modelling and inversion software.

Though promising advances in the technology of logging through metal casing have been made in recent years, the resolution of through-casing measurements is still far inferior to measurements in uncased boreholes. Singer and Dodds (2004) presented a study of the resolution capabilities when using two borehole casings as long cylinder electrodes and measuring the admittance between them. If measurements are stable and have sufficient repeatability, the conductance is a reliable measure of the bulk average conductivity between the boreholes. If the boreholes are not too far from each other and if the change in conductivity is not too small, it should be possible to use the bulk conductance as a monitoring measure. Newmark et al. (1999) demonstrated that some horizontal, but no vertical, resolution can be achieved if multiple cased holes are used as electrodes.

In the case of plastic casing in both holes, monitoring can be done with electromagnetic methods (Wilt et al., 1995). In this case a vertical magnetic dipole source is placed in one borehole and a receiver coil, possibly three-component, in the other. Such measurements have also been conducted with the transmitter in a cased hole and the receiver in an uncased hole with acceptable results, provided that the distance is not too great between the holes (Wilt and Alumbaugh, 1998). For small distances between holes, results can be obtained even with two cased holes. However, electromagnetic methods are much better at detecting conductive anomalies than resistive ones.

The ideal circumstances for electrical monitoring of CO_2 injection would be from uncased boreholes separated by a distance of a few hundred metres, and with electrodes placed over an interval of at least the same length. Though such a set-up would be costly, it is worthwhile examining whether CO_2 storage can be monitored by ERT. At 2 km depth and at a temperature of 95°C, CO_2 will be in a supercritical state with no electrical conductivity. For our models we have assumed an average porosity of 28%, and 30% of the pore space still filled with residual methane. Electrical logs through the formations indicate resistivities of around 3 Ω.m and 8 Ω.m for the reservoir sandstone and surrounding shales respectively.

The present study complements the papers in this issue by Sherlock et al. (2006) and Siggins (2006) concerning the seismic and gravity aspects of the OBPP project.

MODEL SETUP

Electrode arrays

Many different electrode configuration types have been used for ERT. The pole-pole array, where a current electrode is in one hole and a potential electrode is in the other, and one current and one potential electrode are on the surface at "infinity", is widely used. It has a good signal-to-noise ratio, and the number of possible electrode configurations is relatively small, so that it becomes possible to measure an exhaustive set of configurations. The drawback is that it can be logistically difficult to place the two surface electrodes far enough away from the subsurface electrodes and far away from each other. As a rule of thumb, the distance to the far electrodes must be at least 20 times the typical distance between electrodes in the boreholes, and the higher the near-surface resistivity relative to the average resistivity in the subsurface survey area, the more severe the demands on distance to the faraway electrodes. As an example, if the survey area is at a

Cooperative Research Centre for Greenhouse Gas Technologies
CSIRO Petroleum,
26 Dick Perry Avenue,
KENSINGTON, WA
Australia, 6151
Phone: +61 8 6436 8729
Facsimile: +61 8 6436 8729
Email: nbc@geo.au.dk

Manuscript received 25 November, 2005.
Revised manuscript received 16 December, 2005.

depth of 2 km and the distance between boreholes is 200 m, then the faraway electrodes must be at least 6 km away.

The pole-bipole array has two electrodes in one hole and one in the other with one electrode at the surface at "infinity". The signal-to-noise ratio is good, and there is only one far electrode and so fewer logistical problems.

With bipole-bipole arrays, all four electrodes are in the boreholes, most often two in each hole, and there are no problems with far electrodes. However, for certain configurations the signal-to-noise ratio can be very small and the measurements thus of little use.

Zhou and Greenhalgh (2000) have conducted a comprehensive study of the various electrode configuration types, and show that pole-bipole and bipole-bipole configuration types with two current or two potential electrodes in the same hole are problematic because of a low signal-to-noise ratio, and because the measured voltages of some configurations cannot be transformed to apparent resistivity. They conclude that the configuration types useful for ERT are the pole-pole, the pole-bipole, and bipole-bipole configuration types, avoiding configurations with two potential electrodes in the same hole. Sasaki (1992) concludes that the bipole-bipole configuration type is better suited than pole-pole and pole-bipole configuration types in cross-hole surveys.

Studies have shown that it is advantageous to measure not only cross-hole configurations but also configurations with all active electrodes in one hole (Sugimoto, 1999). This improves the resolution of the data set, because it adds important information about the near-borehole regions.

The models

A synthetic modelling example, simulating the basic features of a real monitoring situation, has been carried out using the RES2DMOD and RES2DINV programs (Loke and Barker, 1996). The sequence of four models illustrating an increasing CO_2 content and the electrodes mounted in the borehole are shown in the left hand column of Figures 2 to 5. Two boreholes separated by 200 m, each with 21 electrodes with a unit spacing of 10 m, penetrate the formations into which CO_2 is injected at 2 km depth. The model is simple, but it honours the basic configuration and properties of the Otway Pilot site with a dipping, fault-bounded reservoir and an overlying shale seal. In the initial model, M00, a small methane cap remains post-production. The three subsequent models, M10, M20, and M30, each add 10 m of CO_2 to the initial small pocket of methane. The methane/CO_2 bearing sandstone has been given a resistivity of 100 Ω.m.

The two-dimensional model cells are 10 m × 10 m, from -50 m to 250 m in the horizontal direction and from 2000 m to 2200 m in the vertical direction, for a total of 600 cells. Model cells 50 m outside of the interval between the boreholes have been included in the model. They influence the data, but the sensitivity of most electrode configurations is low for these model cells. To ensure accuracy of the modelling and inversion, the central area of the actual model cells is padded with cells whose size increases with distance from the central area.

The electrode configuration types used

Three different electrode configuration types have been used for the modelling experiment: pole-pole configurations (pp), bipole-bipole configurations with only cross-hole configurations (bb0) and bipole-bipole configuration with both cross-hole configurations and configurations with all electrodes in one borehole (bb1). In the pp configuration type, both cross-hole and in-hole configurations are used for a total of 861 configurations. The cross-hole bb0 and bb1 configuration types have one current and one potential electrode in each hole and all configurations have the current electrode above the potential electrode (no crossed configurations). They consist of all combinations of bipoles of 2 unit electrode separations moved one unit along the boreholes, all combinations of bipoles of 4 unit electrode separations moved 2 units along the boreholes, all combinations of bipoles of 8 unit electrode separations moved 4 units along the boreholes, and the four possible 16 unit bipole combinations. Finally the single possible 20 unit bipoles are used. The bb0 configuration type has a total of 463 configurations. The additional configurations in the bb1 configuration

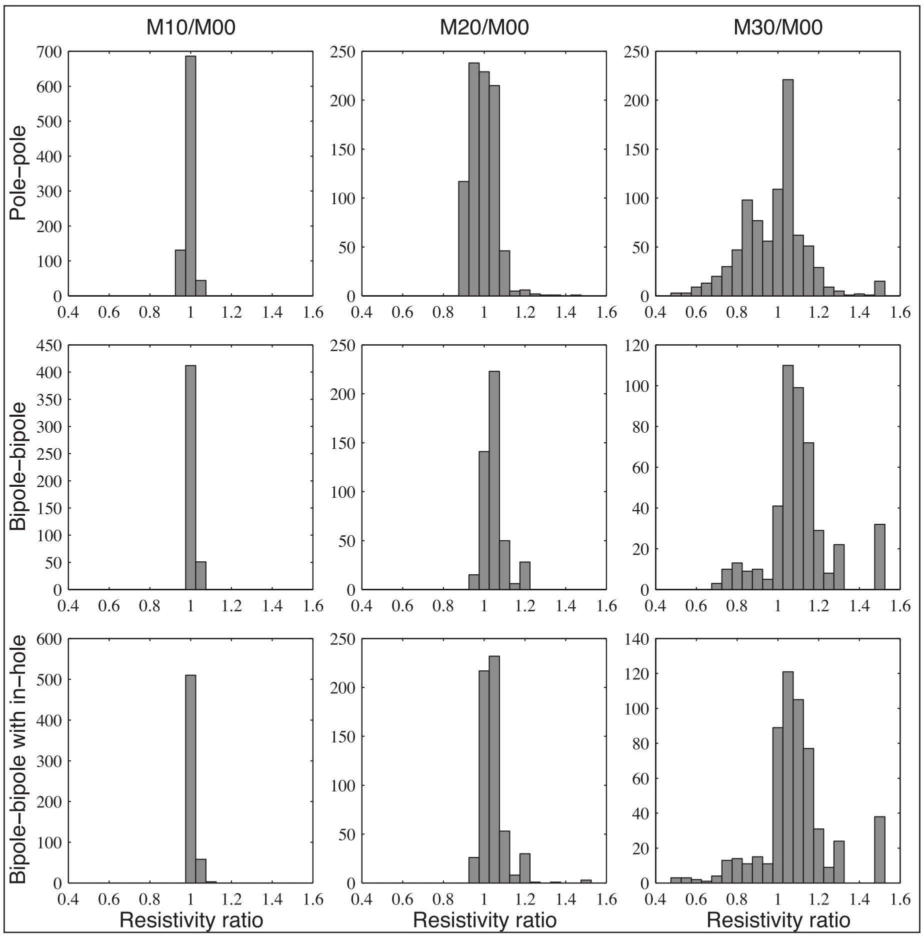

Fig. 1. Histograms of the ratio between the baseline model and the models with increasing CO_2 content. Top row: pole-pole electrode configuration (pp); middle row: bipole-bipole configuration (bb0); bottom row: bipole-bipole plus additional configurations with all electrodes in one hole (bb1).

type with all electrodes in one hole are gradient arrays. The first is a 20 unit current dipole where the 18 possible one-unit potential dipoles between the current electrodes are measured; the next three are 10 unit current dipoles shifted 5 units with the eight possible one-unit potential dipoles between the current electrodes measured; and finally four 5 unit current dipoles shifted 5 units with the three possible one-unit potential dipoles between the current electrodes measured. Naturally, in-hole configurations have been measured in both boreholes.

Sensitivity of the electrode configuration types

To illustrate the sensitivity of the different configuration types, the ratios between the data of the models M10, M20, and M30 and the base line model M00 have been calculated to provide a bulk measure of data changes. These data ratios are presented in Figure 1 as histograms. As expected, the data changes increase with increasing amount of CO_2 in the models. Note also that there are both negative and positive changes to the introduction of a resistive anomaly.

For the M10 model, data changes are small and comparable with measurement noise, and hence it must be expected that the sensitivity is low for this model. For the M20 and M30 models, data changes are noticeable, and the models should be resolvable. The pp, bb0, and bb1 configuration types all have rather similar distributions of data change.

MODELLING AND INVERSION

Forward responses of the four true models for the three sets of electrode configuration types were calculated with the program RES2DMOD using the finite element modelling option. The responses were calculated as apparent resistivities and to increase the accuracy, the responses were normalised with the apparent resistivities of a modelled halfspace. Normally distributed noise of 5% was added to all data.

Data from the four models and the three sets of configuration types: pp, bb0, and bb1, was inverted using both the L2-norm and the L1-norm. The two different optimisations affect not only the weighting of the data, but also the smoothness constraints between neighbouring model cells. The L1-norm, which minimises the absolute jumps in resistivity between neighbouring model cells, gives a more blocky inversion than the L2-norm, which minimises the smoothness of the model. All inversions converged in five iterations with a residual close to the noise level of 5%.

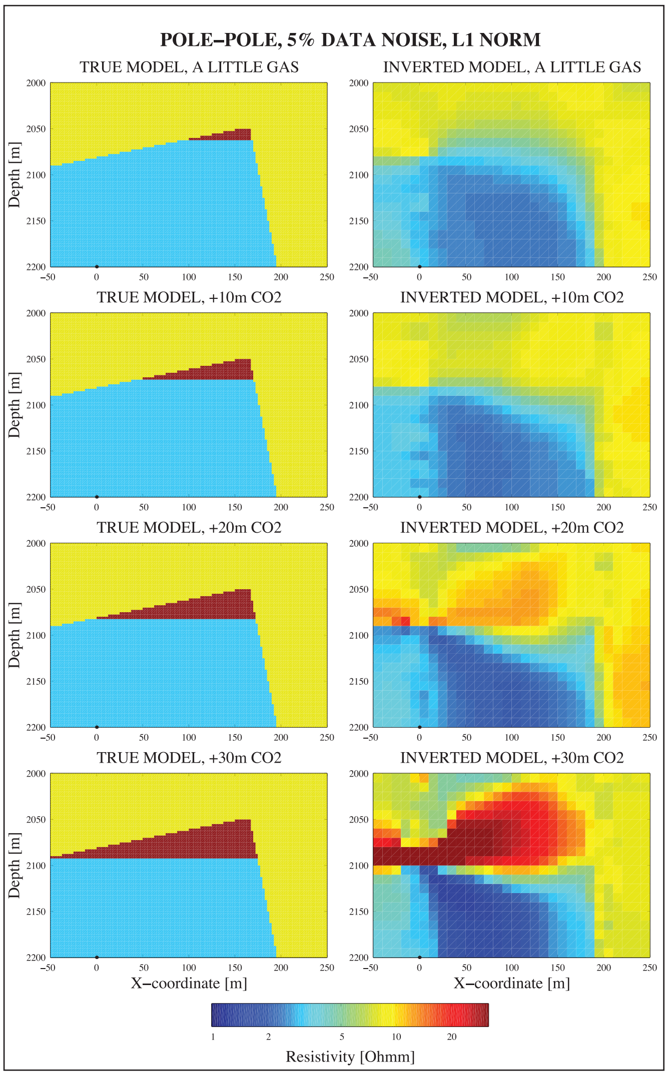

Fig. 2. In the left column is the sequence of four models illustrating an increasing CO_2 content and the borehole configurations used for ERT modelling. The right column shows the inversion results for pole-pole configurations, using the L1-norm.

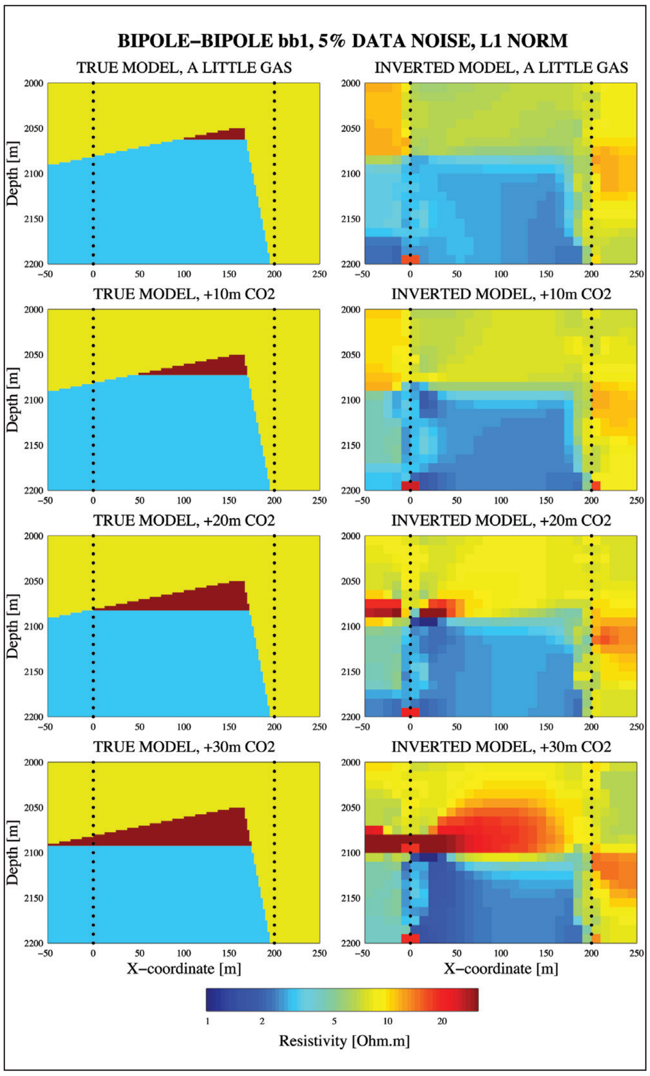

Fig. 3. In the left column is the sequence of four models illustrating an increasing CO_2 content and the borehole configurations used for ERT modelling. The right column shows the inversion results for bipole-bipole configurations with in-hole measurements, using the L1-norm.

RESULTS

In all cases, the L2-norm inversion results appear more smeared than the L1-norm results. The model cells outside the interval between the boreholes are generally poorly determined, and artefacts of the inversion are generally more pronounced for the L2-norm than for the L1-norm. For reasons of space, only the L1-norm inversion results for the pp and bb1 configuration types are shown here. The pp and bb1 inversions shown in Figures 2 and 3 have the smallest artefacts, which is probably due to the in-hole configurations, and they best outline the geometry of the resistive target. All configuration types have problems discerning M10 from M00.

The ratio between the model resistivities of the M10, M20, and M30 models and the base line M00 model will help in the assessment of the different inversion options. Figure 4 and 5 show the ratio plots for the L1-norm inversions in Figure 2 and 3, and the artefacts of the models are significantly diminished.

Calibration of bulk resistivity change

An undesirable effect of the smoothness constraints imposed by all inversion programs is that all resistivity anomalies appear more or less fuzzy-edged, without the sharp boundaries they might actually possess. Also, data noise will introduce artefacts into the resulting models. However, the resistivity change relative to a reference model, integrated over the model elements, could be an interesting bulk measure of the total change in CO_2 contents. The integrated change, S, is defined by

$$S = \sum_{i=1}^{N} a_i \cdot \log_{10}\left(\rho_i / \rho_r\right) , \tag{1}$$

where ρ_i and ρ_r are the resistivities of the inverted model and the reference true model, respectively, and a_i is the area of the i-th cell. Summation is carried out over all N model elements. The integrated resistivity change of the inverted models as a function of the integrated resistivity change of the true models is plotted in Figure 6 for the three configuration types used for inversions with both the L1- and L2-norm. It appears that the total integrated change is a reasonably good measure of the true change, and plots such as Figure 6, derived for appropriate models, could be used to calibrate the total change in CO_2 content from inversion of ERT data. As seen in Figure 6, the plots for the L2-norm are considerably more erratic than for the L1-norm.

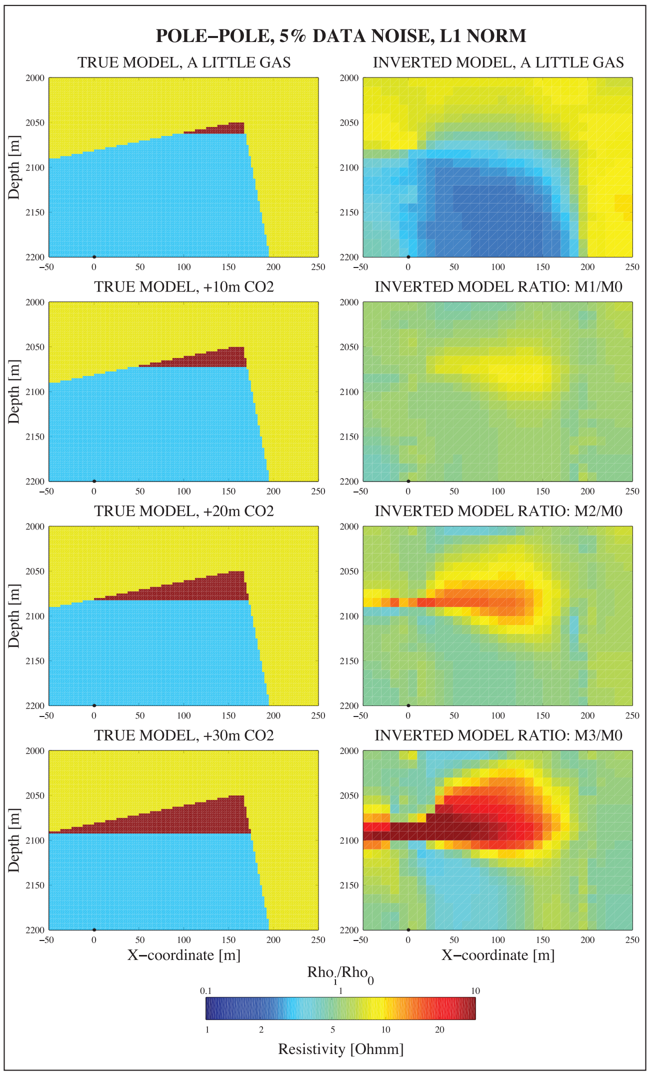

Fig. 4. In the left column is the sequence of four models illustrating an increasing CO_2 content and the borehole configurations used for ERT modelling. The right column shows the ratio between the inversion results for the pole-pole configurations shown in Figure 2, and the background-model result there.

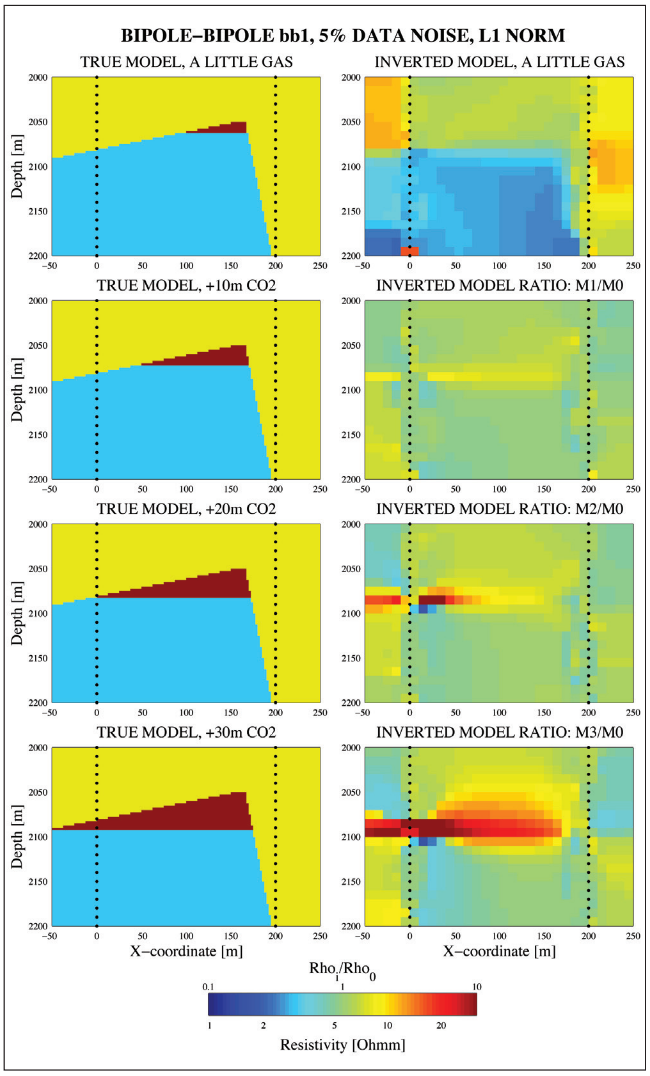

Fig. 5. In the left column is the sequence of four models illustrating an increasing CO_2 content and the borehole configurations used for ERT modelling. The right column shows the ratio between the inversion results for the bipole-bipole configurations with in-hole measurements shown in Figure 3, and the background-model result there.

DISCUSSION AND CONCLUSION

Four issues have not been included in the present preliminary study, but should be pursued in the future: Optimisation of the electrode arrays with respect to the specific resistivity structure of an injection site; inversion with prior information on the inverted models; mutually constrained inversion of time-lapse measurements; and the limitations of the assumption of two-dimensionality.

For any electrode setup, there is a practical limit to how many electrode configurations can be measured in a given time, so which configurations should be measured? It is not a problem to measure all 861 pole-pole configurations, but there are tens of thousands of bipole-bipole configurations, even when imposing the restriction mentioned in the previous section. Curtis and Maurer (2000) argue convincingly for the application of optimisation methodologies to geophysical experiments. However, no optimisation studies focused on the ERT problem have yet been published (Hansruedi Maurer, personal communication), but in Maurer et al. (2000) an example is given on optimal design of a galvanic electric surface electrode array.

In the present preliminary study, prior information was not introduced in the inversions, but it would be natural to include no-change constraints on the parts of the model that are known to be unaffected by the CO_2 injection.

When a series of data sets are available it is possible to invert them all simultaneously. This inversion is done with constraints on the temporal rate of change of resistivity and it will give better estimates of both the background resistivity structure and the changes caused by the CO_2 injection (Barker and Moore, 1998; Loke, 1999).

Despite the simple nature of the models used here to represent CO_2 storage at the Otway Pilot site, a number of useful guidelines can be formulated regarding the applicability of ERT for monitoring the build-up of CO_2 in the reservoir:

Electrodes must be placed permanently in the boreholes within a depth interval at least as great as the distance between the boreholes. Measurements should be repeated at regular intervals with an appropriate set of configurations.

A comprehensive baseline data set must be collected before injection to infer the background resistivity distribution to which all subsequent measurements will be compared. A thorough and up-to-date inversion of this data set is crucial for the success of subsequent monitoring measurements.

Forward modelling and analyses of resolution of the electrode configuration should be carried out on models that include all available geological knowledge, both before the initial measurements and after pre-injection data have been collected.

With the 2 km reservoir depth at Otway there may be special challenges for ERT concerning electrode emplacement and instrumentation.

The results of the modelling show that ERT is capable of detecting, in a conductive environment, resistive changes resulting from CO_2 injection over a certain threshold. The pole-pole and bipole-bipole configuration types with in-hole configurations appear advantageous from a resolution point of view and the integrated change in the logarithm of the resistivity correlates well with the values for the true models. Inversion with the L1-norm produces consistently better results than with the L2-norm. It must be kept in mind that the pole-pole configuration type requires two far electrodes at a distance of at least 20 times the maximum electrode separation, but the bipole-bipole configuration type offers a good alternative.

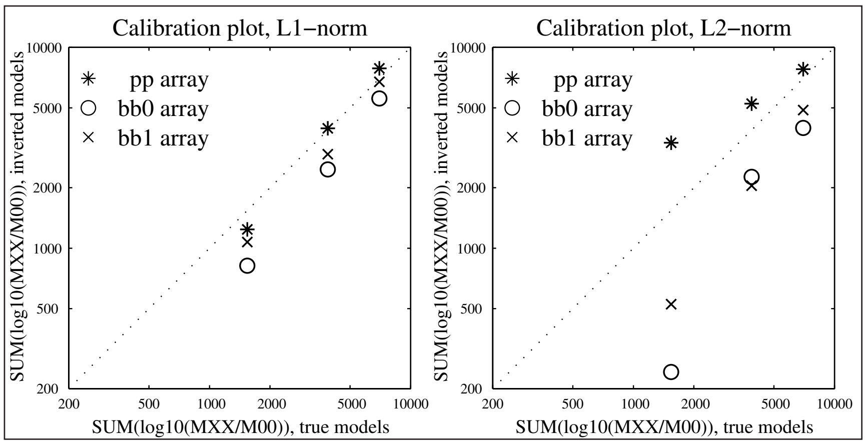

Fig. 6. The integrated resistivity change for the L1-norm and L2-norm inversions for the three electrode configurations as a function of the integrated resistivity change in the true models. The integrated resistivity change is the sum over the models of the logarithm of the change in resistivity.

ACKNOWLEDGMENTS

This work was carried out for the Cooperative Research Centre for Greenhouse Gas Technologies, Storage Program under the Monitoring and Verification Project. Eric Wedepohl, Geoforce, is acknowledged for help with the software.

REFERENCES

Barker, R., and Moore, J., 1998, The application of time-lapse electrical tomography in groundwater studies: *The Leading Edge*, **17**, 1454–1458.

Daily, W., and Ramirez, A.L., 2000, Electrical imaging of engineered hydraulic barriers: *Geophysics*, **65**, 83–94.

Hoversten, G.M., Gritto, R., Washbourne, J., and Daley, T.M., 2003, Pressure and fluid saturation prediction in a multicomponent reservoir using combined seismic and electromagnetic imaging: *Geophysics*, **68**, 1580–1591.

Loke, M.H., and Barker, R.D., 1996, Practical techniques for 3-D resistivity surveys and data inversion: *Geophysical Prospecting*, **44**, 499–523.

Loke, M.H., 1999. Time-lapse resistivity imaging inversion: *Proceedings of the 5th Meeting of the Environmental and Engineering Geophysical Society European Section*.

Newmark, R., Daily, W., and Ramirez, A., 1999, Electrical resistance tomography using steel cased boreholes as electrodes: *69th Annual International Meeting of the Society of Exploration Geophysicists, Expanded Abstracts*, **18**, 327.

Sasaki, Y., 1992, Resolution of resistivity tomography inferred from numerical simulation: *Geophysical Prospecting*, **40**, 453–464.

Sherlock, D.H., Toomey, A., Hoversten, G.M., Gasperikova, E., and Dodds, K.J., 2006, Gravity monitoring of CO_2 storage in a depleted gas field: A sensitivity study: *Exploration Geophysics*, **37**, (this issue).

Siggins, A.F., 2006, Velocity-effective pressure response of CO_2 saturated sandstones: *Exploration Geophysics*, **37**, (this issue).

Singer, B.S., and Dodds, K., 2004, Monitoring electrical properties of rocks in target zone of CO_2 sequestration site: *17th Geophysical Conference and Exhibition of the Australian Society of Exploration Geophysicists, Expanded Abstracts*.

Sugimoto, Y., 1999, Shallow high-resolution 2-D and 3-D electrical crosshole imaging: *The Leading Edge*, **18**, 1425–1428.

Wilt, M.J., Alumbaugh, D.L., Morrison, H.F., Becker, A., Lee, K.H., and Deszcz-Pan, M., 1995, Crosswell electromagnetic tomography: System design considerations and field results: *Geophysics*, **60**, 871–885.

Wilt, M.J., and Alumbaugh, D.L., 1998, Electromagnetic methods for development and production: State of the art: *The Leading Edge*, **17**, 487.

Zhou, B., and Greenhalgh, S.A., 2000, Cross-hole resistivity tomography using different electrode configurations: *Geophysical Prospecting*, **48**, 887–912.

孔井間比抵抗トモグラフィによる CO_2 圧入モニタリング

N.B. クリステンセン[1]・D. シャーロック[1]・K. ドッズ[1]

要　旨：　本研究では、CO_2 圧入モニタリングにおける比抵抗トモグラフィ(ERT)の解像力を検討する。比抵抗トモグラフィは、CO_2 プリュームを挟んで存在する 2 本のケーシングなしの坑井を使用して、ポール・ポール法とバイポール・バイポール法の電極配置で実施された。圧入前の初期モデルとそれに続く 3 段階の CO_2 圧入後のモデルを 2 つの電極配置それぞれについて計算し、ノイズを加えて理論データとした。このデータを入力として、L1、L2 ノルムの両方を最適化するインバージョンをおこなった。

その結果、ある閾値以上の体積の CO_2 を確実に検出することができることが示された。 L1-最適化は L2-最適化より多くの場合優れていると判明した。注入前のモデルのインバージョン結果を用いて、各圧入ステージのインバージョン結果を正規化することによって、比抵抗変化部の良いイメージが得られた。また、比抵抗変化の総量の総合的測定が、圧入した CO_2 の総体積の測定に有効であることが証明された。

キーワード：CO_2 地層処分、比抵抗トモグラフィ、モニタリング

시추공간 전기비저항 토모그래피를 이용한 CO_2 주입 모니터링

N.B. Christensen[1], D. Sherlock[1] and K. Dodds[1]

요　약：　이 연구에서는 CO_2 주입 모니터링에서의 전기비저항 토모그래피(ERT)의 분해능에 대해 조사한다. CO_2 주입체 양쪽의 케이싱 없는 시추공에서 단극자 및 양극자 전극 배열이 사용된다. 주입 전 및 주입에 따른 3 단계 모델에 대한 반응이 계산되고, 잡음이 더해진 후의 이론 값들이 L1 과 L2 norm 을 사용해 역산된다.

역산결과는 어느 정도 수준이상의 CO_2 부피가 확실히 감지됨을 보여준다. 대부분의 경우에 L1 norm 의 경우가 L2 에 비해 우월함이 판명되었다. 역산 결과를 주입 전 모델의 역산결과로 정규화하면 전기비저항이 변화하는 부분의 훌륭한 영상을 보여주며, 비저항의 전체적인 변화를 통합해서 판단하면 전체 주입된 부피에 대한 타당한 측정이 이루어짐이 입증된다.

주요어：CO_2 격리, 전기비저항 토모그래피, 모니터링, 모형 연구

温暖化ガス技術共同研究センター
1 オーストラリア連邦科学産業研究機構
CSIRO Petroleum, 26 Dick Perry Avenue, KENSINGTON, WA, Australia 6151

Cooperative Research Centre for Greenhouse Gas Technologies
1 CSIRO Petroleum